

A Novel Mechanism for Reactions of Thiirane with the Thiirane Radical Cation. An Experimental and *ab Initio* Study

Scott Ekern,[†] Andreas Illies,^{*} Michael L. McKee,^{*} and Michael Peschke

Contribution from the Department of Chemistry, Auburn University, 179 Chemistry Building, Auburn University, Alabama 36849-5312

Received July 26, 1993^{*}

Abstract: An experimental and computational study of the ion–molecule reactions initiated by the reaction of SC_2H_4^+ with SC_2H_4 has been carried out. The dimer ion is observed in a hybrid drift tube/ion source under chemical ionization conditions at low temperatures and high pressures. However, the ion intensity is much lower than expected for a product containing a stable two-center three-electron (2c-3e) S...S bond. Above room temperature, ion intensities for m/z 92 $\text{S}_2\text{C}_2\text{H}_4^+$, m/z 124 $\text{S}_3\text{C}_2\text{H}_4^+$, m/z 156 $\text{S}_4\text{C}_2\text{H}_4^+$, and m/z 184 $\text{S}_4\text{C}_4\text{H}_8^+$ dominate. The first three ions result from sequential association of SC_2H_4^+ with SC_2H_4 followed by elimination of ethylene, while the latter ion (m/z 184) is due to the association of $\text{S}_3\text{C}_2\text{H}_4^+$ with SC_2H_4 without loss of ethylene. As the temperature is lowered, clustering is promoted relative to reaction channels involving loss of ethylene. The experimental results are not in full agreement with a published *ab initio* study which found that the product channel was 33-kJ/mol endothermic with respect to reactants. The present *ab initio* calculations indicate that another reaction channel is possible, resulting in a four-membered-ring $c\text{-S}_2\text{C}_2\text{H}_4^+$, which is exothermic by 43.0 kJ/mol. The potential energy surface for this channel, including transition states, was computationally studied in detail. An interesting aspect of this mechanism is the stepwise addition of sulfur atoms forming successively larger rings which continues until the six-membered-ring $\text{S}_4\text{C}_2\text{H}_4^+$ is formed.

Introduction

Historically, ion–molecule reactions have been of great interest to chemists. Many kinetic, dynamic, and mechanistic studies have been made involving numerous types of reactions and molecules. Studies of gas-phase ions have led to some of the exciting breakthroughs in chemistry, for example the recent discovery of C_{60} .¹ Ions are also implicated in the synthesis of planetary and interstellar molecules.² Recently our group has had an interest in two-center three-electron, 2c-3e or $(\sigma)^2(\sigma^*)^1$, bonding in ion–molecule reaction products. We have determined the experimental gas-phase S...S bond enthalpy in $[(\text{Me})_2\text{S}\cdots\text{S}(\text{Me})_2]^+$ and $[(\text{Et})_2\text{S}\cdots\text{S}(\text{Et})_2]^+$ to be 110 and 115 kJ/mol, respectively, and estimated the I...I bond in $\text{CH}_3\text{I}\cdots\text{ICH}_3^+$ to be in the range of 96–109 kJ/mol.³ The molecular interaction in 2c-3e bonding can be illustrated by the simple molecular orbital picture below.

Such bonds have been extensively studied in solution by pulse radiolysis experiments.⁴ However, very little experimental data on the bonding interactions exist. On the basis of published theoretical results⁵ summarized in Figure 1, we initiated a study to determine the S...S 2c-3e bond strength in the ionized thiirane

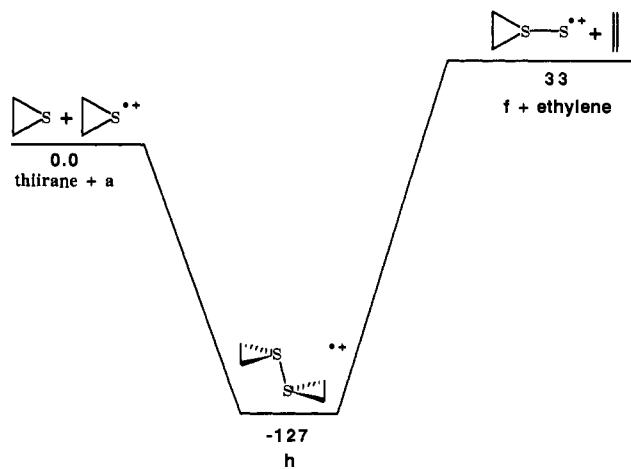
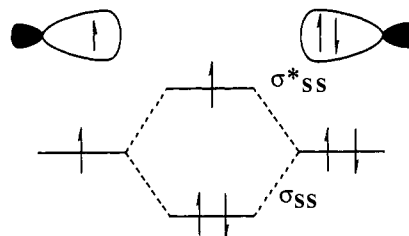


Figure 1. Schematic potential energy diagram reported by Gill et al.⁵ Energies are in kJ/mol.



dimer $[c\text{-C}_2\text{H}_4\text{S}\cdots c\text{-SC}_2\text{H}_4]^+$. Experimentally, ion–molecule equilibrium constants are determined as a function of temperature which allows the enthalpy and entropy of binding to be extracted from the van't Hoff equation:⁶

(6) Keesee, R. G.; Castleman, A. W., Jr. *J. Phys. Chem. Ref. Data* 1986, 15, 1011.

[†] Authors are in alphabetical order.

^{*} Abstract published in *Advance ACS Abstracts*, December 1, 1993.

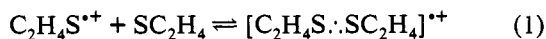
(1) Kroto, H. W.; Heath, J. R.; O'Brien, S. C.; Curl, R. F.; Smalley, R. E. *Nature* 1985, 318, 162.

(2) Smith, D. *Chem. Rev.* 1992, 92, 1473.

(3) (a) Illies, A. J.; James, M. A.; McKee, M. L.; Peschke, M.; Ying, D. To be submitted for publication. (b) Illies, A. J.; Livant, P.; McKee, M. L. *J. Am. Chem. Soc.* 1988, 110, 7980. (c) Livant, P.; Illies, A. J. *J. Am. Chem. Soc.* 1991, 113, 1510.

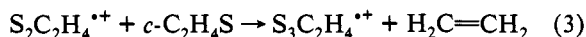
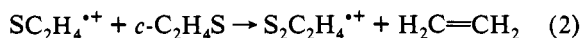
(4) For leading references see: (a) Asmus, K.-D. In *Sulfur-Centered Reactive Intermediates in Chemistry and Biology*; Chatgililoglu, C., Asmus, K.-D., Eds.; Plenum Press: New York and London, 1990; p 155. (b) Gilbert, B. C. In *Sulfur-Centered Reactive Intermediates in Chemistry and Biology*; Chatgililoglu, C., Asmus, K.-D., Eds.; Plenum Press: New York and London, 1990; p 135.

(5) Gill, P. M. W.; Weatherall, P.; Radom, L. *J. Am. Chem. Soc.* 1989, 111, 2782.

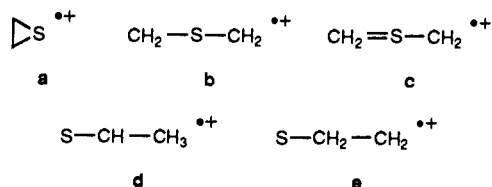


$$\ln K_p = -\Delta H^\circ_{rxn}/RT + \Delta S^\circ_{rxn}/R \quad (I)$$

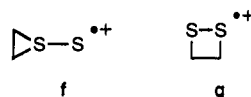
The gas-phase ion-molecule chemistry of thiirane has been explored by Baykut et al.⁷ In a pair of ICR studies they reported peaks at m/z 60, 92, 124, and 156 which they attributed to the molecular formulas $SC_2H_4^{*+}$, $S_2C_2H_4^{*+}$, $S_3C_2H_4^{*+}$, and $S_4C_2H_4^{*+}$. They proposed the sulfur transfer reactions 2-4 to account for the peaks at m/z 92, 124, and 156.



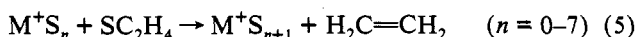
From reactivity data the authors concluded that the parent thiirane radical cation was the three-membered ring isomer, **a**, rather than the alternative structures: **b**, **c**, **d**, or **e**.



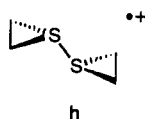
This conclusion was later supported by Gill et al.⁵ from *ab initio* calculations on the thiirane radical cation and indirectly by Fowler et al.⁸ with calculations on the neutral thiirane molecule. Further reactivity information on the secondary ion $S_2C_2H_4^{*+}$ led to the tentative conclusion that structure **f** was more probable than **g** for $S_2C_2H_4^{*+}$.



Sulfur transfer reactions similar to reactions 2-4 were also suggested by Carlin et al.⁹ for the reaction of ionized metal-sulfur complexes ($M = Fe^+$, Co^+ , V^+ , and Ti^+) with thiirane (reaction 5):



Later, Qin et al.¹⁰ studied the chemistry of thiirane using an ESR radiolysis matrix isolation technique and reported experimental evidence for the existence of **h**. Reaction 2 was suggested to explain the observed postirradiation evolution of ethylene.



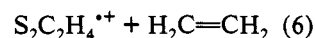
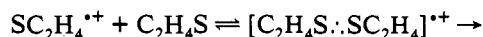
The dimer cation (**h**) formed in reaction 1 is the ion we initially intended to study. Since the signal assigned to **h** in the Freon matrices was found to disappear at temperatures above 105 K, it was concluded that **h** was a reactive intermediate, which reacted further as shown below:

(7) (a) Baykut, G.; Wanczek, K.-P.; Hartmann, H. *Adv. Mass Spectrom.* **1980**, *8A*, 186. (b) Baykut, G.; Wanczek, K.-P.; Hartmann, H. In *Dynamic Mass Spectroscopy*; Price, D., Todd, J. F. J., Eds.; Heyden and Son: London, 1981; Vol 6, pp 269-283.

(8) Fowler, J. E.; Alberts, I. L.; Schaefer, H. F. *J. Am. Chem. Soc.* **1991**, *113*, 4768.

(9) Carlin, T. J.; Wise, M. B.; Freiser, B. S. *Inorg. Chem.* **1981**, *20*, 2745.

(10) Qin, X. Z.; Meng, Q.-C.; Williams, F. J. *Am. Chem. Soc.* **1987**, *109*, 6778.



Ab initio calculations were carried out by Gill et al.⁵ on the $(c-C_2H_4S)_2^{*+}$ potential energy surface at the MP2/6-31G**//6-31G* level. They found that structure **h** was 127 kJ/mol more stable than the reactants, $SC_2H_4^{*+}$ and C_2H_4S , and 160 kJ/mol more stable than the proposed products, $S_2C_2H_4^{*+}$ and C_2H_4 . However, the results of Gill et al.⁵ do not appear to be consistent with experiment. Firstly, if structure **h** is calculated to be in a potential energy minimum that is 127 kJ/mol deep, then why was it not observed in the ICR experiments by Baykut et al.⁷ Secondly, why does reaction 2 appear to proceed at liquid nitrogen temperatures in the matrix isolation experiments, if the products are 33 kJ/mol endothermic? These questions led us to consider whether the potential energy surface depicted in Figure 1 was correct. New high-pressure mass spectra and more extensive *ab initio* calculations reported here provide a much more complete understanding of the thiirane radical cation reactions.

Experimental Method

The ion-molecule reactions were studied in our highly modified DuPont mass spectrometer with a new hybrid drift tube/ion source.¹¹ Thiirane, purchased from Aldrich, was outgassed by repeated freeze-pump-thaw cycles and dried over 3 Å molecular sieve. Spectra were taken with ionizing electron energies in the range of 8.5-13 eV in Kr bath gas at total ion-source pressures ranging from 0.10 to 0.25 Torr and compositions ranging from 2 to 5% thiirane. The ion-source temperature was varied by passing cooled or heated dried air through thermal transport channels in the ion-source main block. The temperature, which ranged from 193 to 363 K, was measured both with a platinum resistance thermometer coated with a vacuum-compatible heat transfer grease inserted into a hole in the block and with a Chromel/Alumel thermocouple bolted onto the block. The two independent methods for measuring temperature agreed to within 1 K.

Computational Method

All *ab initio* calculations were carried out using the GAUSSIAN 92¹² and GAMESS¹³ program packages. Geometries were first preoptimized using AM1¹⁴ and PM3¹⁵ then fully optimized (within the appropriate point group) at the UHF/6-31G* level. For several structures, additional optimizations at the UMP2/6-31G* level were carried out. Vibrational frequencies were calculated at the UHF/6-31G* level in order to make zero-point corrections (0.9 weighting factor) and to determine the nature of the potential energy surface. Single-point calculations were carried out at the PMP2/6-31G* level (the P indicates that the effects of spin contamination have been projected out of the MP correlation energies¹⁶) for all UHF/6-31G* optimized geometries. For several structures, PMP4/6-31G* single-point calculations were also carried out at UHF/6-31G* geometries. Optimizations at the UMP2/6-31G* level were followed by single-point calculations at the PMP2 and PMP4/6-31G* levels. Unless otherwise indicated, discussions will refer to our standard level, PMP2/6-31G**//UHF/6-31G**+ZPC. Total energies (hartrees), zero-point energies (kJ/mol), and spin-squared values are presented in Table I while relative energies (kJ/mol) are given in Table II. Geometric parameters are given for optimized geometries in Figure 3. The spin-squared values for several structures in Table I substantially exceed the expected value for a doublet ($\langle S^2 \rangle = 0.75$) and must be viewed with caution. The structure with the highest degree of spin contamination

(11) Ekern, S. P.; Ying, D.; Snowden, K. J.; McKee, M. L.; Illies, A. J. *J. Phys. Chem.* **1992**, *96*, 10176.

(12) Gaussian 92, Revision C, M. J. Frisch, G. W. Trucks, M. Head-Gordon, P. M. W. Gill, M. W. Wong, J. B. Foresman, B. G. Johnson, H. B. Schlegel, M. A. Robb, E. S. Replogle, R. Gomperts, J. L. Andres, K. Raghavachari, J. S. Binkley, C. Gonzalez, R. L. Martin, D. J. Fox, D. J. DeFrees, J. Baker, J. J. P. Stewart, and J. A. Pople, Gaussian, Inc.: Pittsburgh, PA, 1992.

(13) Schmidt, M. W.; Baldridge, K. K.; Boatz, J. A.; Jensen, J. H.; Koseki, S.; Gordon, M. S.; Nguyen, K. A.; Windus, T. L.; Elbert, S. T. *GAMESS. QCPE Bull.* **1990**, *10*, 52.

(14) AM1: Dewar, M. J. S.; Zoebisch, E. G.; Healy, E. F.; Stewart, J. J. P. *J. Am. Chem. Soc.* **1985**, *107*, 3902.

(15) PM3: (a) Stewart, J. J. P. *J. Comput. Chem.* **1989**, *10*, 209. (b) Stewart, J. J. P. *Comp. Aided Mol. Design.* **1990**, *4*, 1.

(16) (a) Sosa, C.; Schlegel, H. B. *Int. J. Quantum Chem.* **1986**, *29*, 1001. (b) Schlegel, H. B. *J. Chem. Phys.* **1986**, *84*, 4530.

Table I. Total Energies (hartrees^a) of All Species Calculated

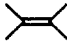

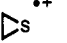
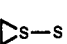
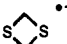
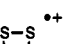
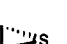
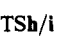
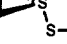
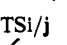
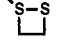
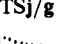

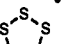
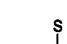

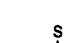


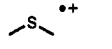
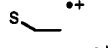
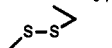
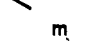
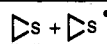
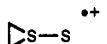

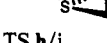
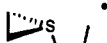
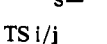
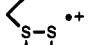
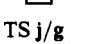

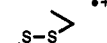
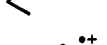
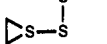
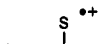
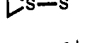
condensed structure	sym	state	//HF/6-31G*				//MP2/6-31G*	
			HF/6-31G*	PMP2/6-31G*	ZPE ^b	$\langle S^2 \rangle^c$	PMP2/6-31G*	PMP4/6-31G*
 ethylene	D_{2h}	1A_g	-78.031 72	-78.284 35	143.8 (0)	0.00		
 thiirane	C_{2v}	1A_1	-475.546 81	-475.928 82	156.0 (0)	0.00	-475.929 23	-475.975 66
 a	C_{2v}	2B_1	-475.260 08	-475.614 54	154.4 (0)	0.76	-475.615 25	-475.663 83
 f	C_s	$^2A''$	-872.769 36	-873.244 16	161.2 (0)	0.76		
 l	C_{2v}	2B_1	-872.754 53	-873.255 56	163.1 (0)	0.77		
 g	C_{2v}	2A_2	-872.783 43	-873.274 85	165.1 (0)	0.77		
 h	C_{2h}	2B_u	-950.833 34	-951.592 69	316.3 (0)	0.78		
 TSb/i	C_1	2A	-950.785 39	-951.519 81	304.5 (1)	1.46		
 i	C_1	2A	-950.821 79	-951.558 64	308.3 (0)	0.76		
 TSj/j	C_1	2A	-950.788 89	-951.536 62	308.7 (1)	1.00	-951.539 85	-951.634 66
 j	C_1	2A	-950.827 72	-951.562 62	313.4 (0)	0.76		
 TSj/g	C_1	2A	-950.814 69	-951.558 48	310.6 (1)	0.92		
 k	C_1	2A	-950.850 23	-951.588 70	320.6 (0)	0.76		
 o	C_2	2A	-1270.310 59	-1270.930 54	171.3 (0)	0.76		
 n'	C_s	$^2A''$	-1270.287 54	-1270.891 71	166.0 (1)	0.76		
 n	C_1	2A	-1270.288 73	-1270.891 99	166.4 (0)	0.76		
 p	C_1	2A	-1667.798 38	-1668.522 29	171.2 (0)	0.76		
 p'	C_s	$^2A''$	-1667.785 37	-1668.510 78	170.3 (2)	0.76		
 q	C_2	2A	-1667.791 40	-1668.540 52	173.6 (1)	0.78		

Table I (Continued)

condensed structure	sym	state	//HF/6-31G*			$\langle S^2 \rangle^c$	//MP2/6-31G*	
			HF/6-31G*	PMP2/6-31G*	ZPE ^b		PMP2/6-31G*	PMP4/6-31G*
	C_{2v}	2A_2	-475.246 01	-475.594 26	142.0 (0)	1.03		
	C_s	$^2A'$	-475.199 91	-475.528 41	143.3 (1)	0.76		
	C_i	2A	-950.750 91	-951.505 46	307.3 (1)	0.85		
								

^a 1 hartree = 2625.5 kJ/mol. ^b Scaled (0.9 factor) zero-point energy (kJ/mol) and number of imaginary frequencies in parentheses. ^c Spin-squared value. Expected value for a doublet is 0.75.

Table II. Relative Energies (kJ/mol) of the Most Germane Structures

lbl	condensed structure	//HF/6-31G*			//MP2/6-31G*		
		HF	PMP2	+ZPC ^b	PMP2	PMP4	+ZPC ^b
		0.0	0.0	0.0	0.0	0.0	0.0
f + C ₂ H ₄		13.4	39.0	34.1			
h		-69.4	-129.5	-124.2			
i	TS h /i 	56.4 -39.1	61.8 -40.1	56.5 ^c -42.0			
j	TS i /j 	47.3 -54.7	17.7 -50.6	16.2 -47.9	12.2	12.7	11.2
g + C ₂ H ₄	TS j /g 	-20.5 -21.7	-39.7 -41.6	-39.5 -43.0			
m		147.0	99.5	96.7			
n , C ₁		0.0	0.0	0.0			
n' , C _s		3.1	0.7	0.3			
o		-57.4	-101.2	-96.8			
p , C ₁		0.0	0.0	0.0			
p' , C _s		34.2	30.2	29.4			
q		18.3	-47.9	-45.7			
k		-113.8	-119.0	-108.0			

^a 1 hartree = 2625.5 kJ/mol. ^b Zero-point correction has been made using UHF/6-31G* frequencies. ^c At the PMP4/6-31G*/6-31G* + ZPC level the relative energy becomes 51.7 kJ/mol. At the CAS(3×3)/6-31G*/6-31G* + ZPC level the relative energy becomes 58.2 kJ/mol.

($\langle S^2 \rangle = 1.46$) was also calculated at the MCSCF level with a 3 electrons in 3 orbitals complete active space (CAS(3×3)/6-31G*). In our notation boldface letters refer to minima and transition states are referred to as TSa/b which would be the transition state between a and b.

Results and Discussion

Experimental Results. Representative experimental mass spectra at three temperatures ranging from 311 to 217 K are

shown in Figure 2. Beginning at 311 K, it is clear that peaks at m/z 60 and 120 are absent and that a peak at m/z 120 grows in as the temperature is lowered. The reaction of m/z 60 with thiirane should form an adduct at m/z 120, the stable 2c-3e bonded structure **h**, yet at the higher temperatures m/z 120 is absent and m/z 60 is never observed at the high ion-source pressures. In other experiments (not shown) at ion-source pressures approaching

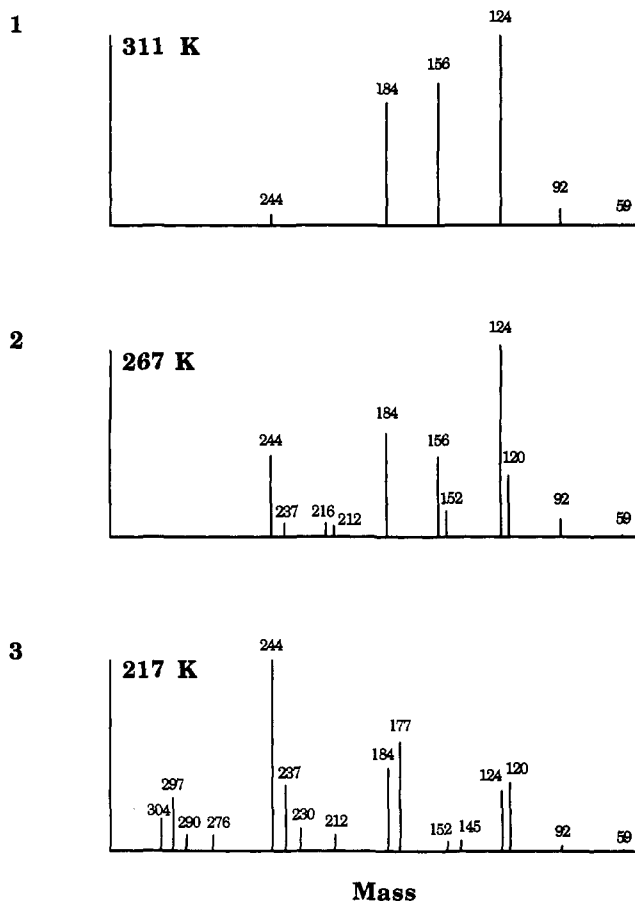
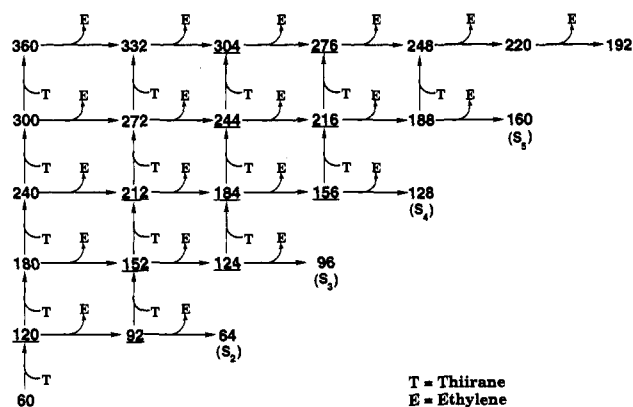


Figure 2. Reconstructed experimental mass spectra as a function of ion source temperature.

Scheme I



normal electron-impact pressures and at low ionizing-electron energies, the mass spectrum has an intense peak at m/z 60. This observation indicates that the m/z 60 intensity is absent in the high-pressure mass spectra shown in Figure 2 due to ion-molecule depletion reactions. Clearly a competing irreversible reaction path exists which drains the m/z 60 intensity, thereby making it impossible to study reaction 1.

Products of association reactions such as m/z 120 are formed initially in excited vibrational states and must be stabilized by third-body collisions. The lifetimes of the excited product ions and the collision rate determine the number of successful stabilizations and hence the ion intensities. m/z 120 was not observed in the ICR studies where pressures are on the order of 10^5 to 10^6 times lower (with corresponding lower collision rates) than in the high-pressure mass spectrometer studies. m/z 120 was also not observed in our high-pressure mass spectrometer

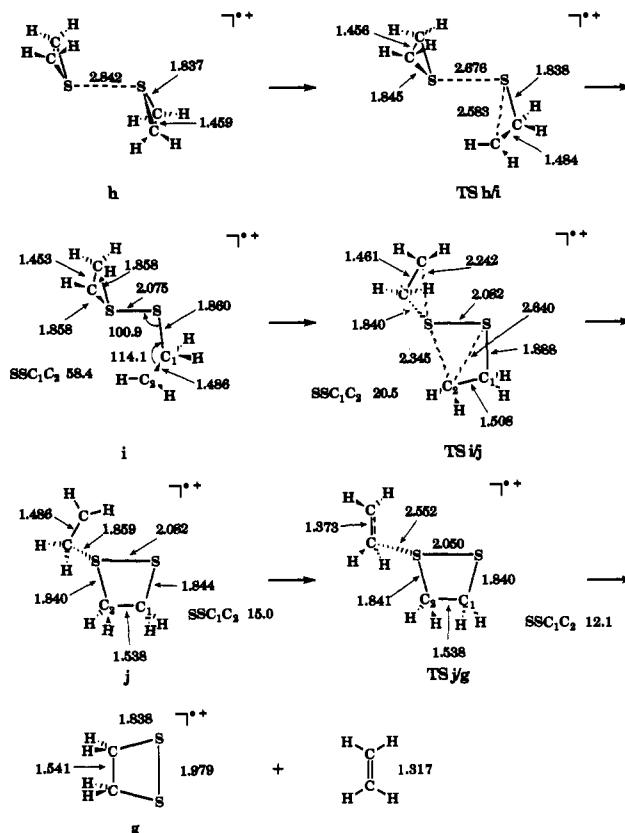


Figure 3. Reaction scheme showing all stable structures and all transition states for the reaction resulting in m/z 92.

studies at the higher temperatures where the lifetimes are expected to be shorter due to the increased thermal energies.

At 311 K and high pressures, the most prominent peaks are m/z 92, 124, 156, and 184. As illustrated in Scheme I for the high-pressure mass spectra, clustering with thiirane occurs as one moves up the scheme and loss of ethylene occurs as one moves across to the right. Underlined numbers represent observed masses. The peak at m/z 92, the product of reaction 2, involves loss of ethylene but *cannot correspond to the endothermic product in Figure 1* since the product (f) plus ethylene are endothermic by 33 kJ/mol and the reaction is not expected to be thermally driven ($1/2RT_{363K} = 1.51$ kJ/mol). The peaks at m/z 124 and 156 arise from sequential reaction of m/z 92 with thiirane and loss of ethylene. The m/z 184 peak results from clustering of m/z 124 with thiirane without loss of ethylene. Hence, stable adduct formation leading to m/z 184 competes with the loss of ethylene from m/z 184 to form 156. Since the m/z 184 peak (assigned to $S_4C_4H_8^+$) has 42 vibrational modes, one expects that it would have a sufficiently long lifetime for effective stabilization.

As one goes to lower temperatures in Figure 2, the most prominent changes in the mass peaks involve the appearance of m/z 120 (the S...S bonded dimer), the disappearance of m/z 156, and the appearance of m/z 152, 212, and 244. At 217 K, m/z 276 and 304 make their appearance and m/z 244 is the most intense peak. At the lowest temperature studied, 193 K, m/z 212 is also relatively intense. In Scheme I these peaks correspond to increased clustering (moving up in the scheme rather than up and to the right). This interpretation is consistent with increased association and decreased elimination at lower temperatures.

At 217 K a few peaks not in Scheme I also appear. These peaks, m/z 145, 177, 230, 237, 290, and 297, suggest that the larger clusters may undergo other reactions too. We have not succeeded yet in identifying these peaks nor in elucidating a mechanism for their formation. It is curious that these peaks are in multiples of seven mass units from peaks in Scheme I.

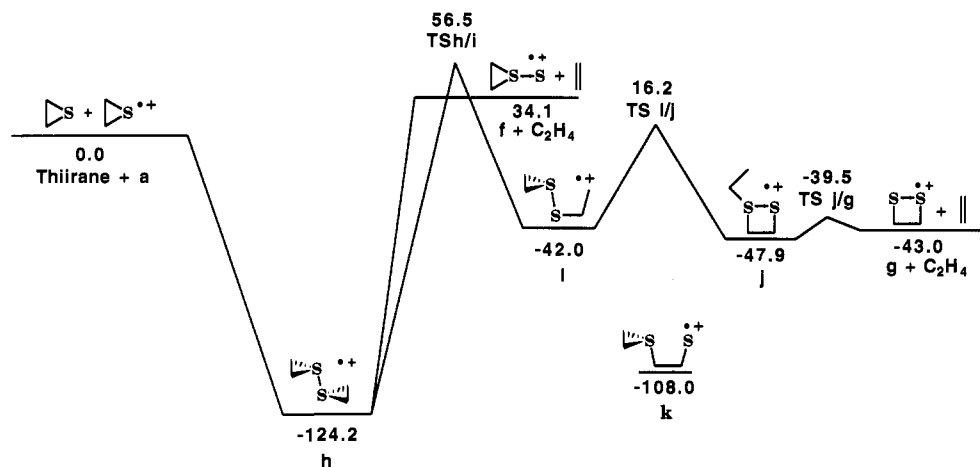


Figure 4. Potential energy surface for the reaction of SC_2H_4 with $SC_2H_4^+$ at the PMP2/6-31G**//6-31G*+ZPC level. The structure of intermediates and transition state are given in Figure 3. Energies are in kJ/mol.

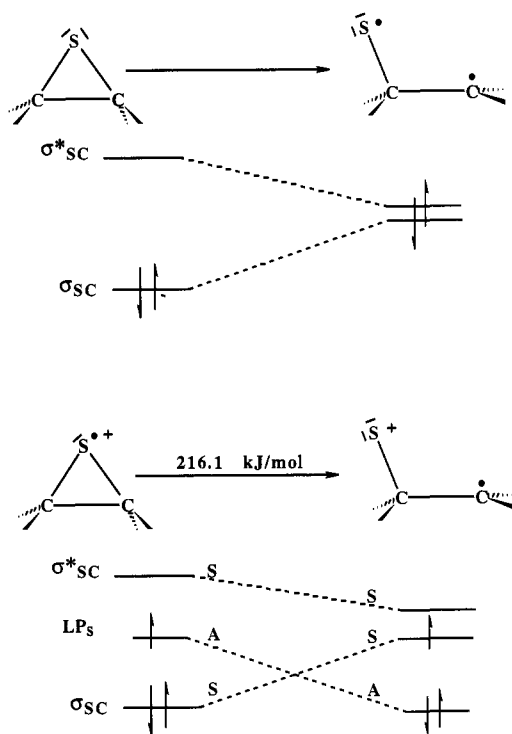


Figure 5. Schematic molecular orbital correlation diagram for the thirane neutral and the thirane radical cation ring-opening transition state.

The mass spectra also provide a few clues about the structure for m/z 92. Since the originally proposed structure **f** for m/z 92 results from an endothermic reaction, one would expect to observe an abundant ion intensity for the parent cation at m/z 60 and for the S:S bonded dimer at m/z 120 as the equilibrium in reaction 1 is established. Yet m/z 120 is observed only at low temperatures and m/z 60 is not observed at all. This result, along with the fact that m/z 92 is observed under all conditions, suggests a different structure for m/z 92 through which the ion intensity of m/z 60 and 120 is drained. Much of the remainder of this paper is devoted to an exothermic reaction mechanism leading to m/z 92.

Computational Results. Structures on the reaction surface $SC_2H_4 + SC_2H_4^+$ are arranged into a mechanistic scheme which is shown in Figure 3 and a potential energy surface which is shown in Figure 4.¹⁷ An important observation is that a pathway for reaction 6 involving ring-closed thirane leading to m/z 92 has

(17) Note that our calculated value for intermediate **f** is slightly larger than the value Gill et al.⁵ obtained since it was obtained with a different method (PMP2/6-31G**//HF/6-31G* vs MP2/6-31G**//HF/6-31G*).

been found for which all the intermediate minima and the final product (**g** + ethylene) are lower in energy than reactants.

The first step is opening one thirane ring of the reactant dimer cation. Before proceeding to a description of the first transition state, we will present a qualitative analysis of the S-C ring opening of ionized thirane since it will be relevant to our later discussion. The most stable structure for both neutral thirane and thirane cation is the closed-ring form.^{5,7,8,18} In neutral thirane the S-C bond is weaker than the C-C bond, and we expect that the bond strengths in ionized thirane would follow the same order. Therefore, the S-C bond will be most easily broken. The unpaired electron in ionized thirane (2B_1 state) is in a sulfur orbital perpendicular to the molecular plane. If the molecular plane of symmetry is conserved as the S-C bond is broken (Figure 5), an orbital crossing occurs between the unpaired electron (A) and the symmetric S-C bonding orbital (S). While a forbidden reaction in the normal application of conservation of orbital symmetry¹⁹ involves the crossing of occupied and empty molecular orbitals, the same rules should apply for the crossing of singly and doubly occupied orbitals. Therefore, the ring opening should be accompanied by an activation barrier and the transition state would not be expected to have a plane of symmetry (breaking the plane of symmetry would allow the symmetric and antisymmetric orbitals to mix, thereby reducing the barrier).

If the ring opening occurs in the thirane dimer (**h**) rather than in ionized thirane, the unpaired electron is in an antibonding S-S σ^* orbital, which is approximately perpendicular to the SCC three-membered rings (Figure 6). While no element of symmetry is conserved as the reaction proceeds, there is an intended crossing between the orbital containing the unpaired electron and the S-C bonding orbital. In the product, the S-C bonding orbital is converted into an orbital located mainly on the terminal methylene which becomes singly occupied. The S-S σ^* orbital, which initially is occupied by one electron, is vacant in the product, increasing the formal bond order of the S-S bond from 0.5 to 1.0. As the transition state is approached, three orbitals, which are required to hold a total of three electrons, should be close in energy. The transition state was located at the UHF/6-31G* level and, as expected, the wave function was heavily spin contaminated ($\langle S^2 \rangle = 1.46$). The S-S bond has shortened somewhat (2.842 \rightarrow 2.676 Å) while the S-C bond has lengthened

(18) The results on the stable forms of thirane neutral and thirane cation can be contrasted with those of oxirane neutral and oxirane cation where disagreement exists as to whether the cation is ring opened or closed. Lindgren, M.; Shiotani, M. In *Radical Ionic Systems. Properties in Condensed Phases*, Lund, A., Shiotani, M., Eds.; Kluwer Academic Publishers: Dordrecht/Boston/London, 1991; pp 128-129.

(19) Woodward, R. B.; Hoffmann, R. *Angew. Chem., Int. Ed. Engl.* 1969, 8, 781.

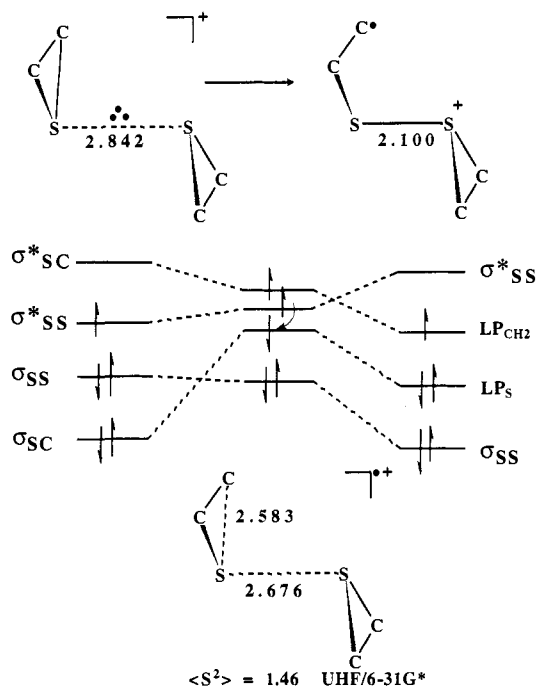


Figure 6. Schematic molecular orbital correlation diagram for the ring-opening transition state (TSg/h).

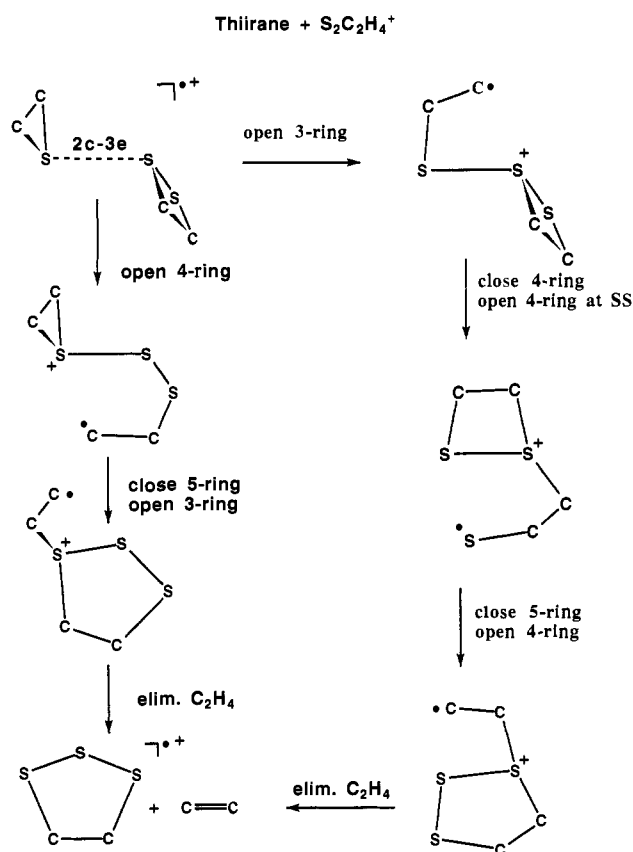


Figure 7. Reaction scheme showing two possible routes from the four-membered ring to the five-membered ring.

considerably (1.837 \rightarrow 2.583 Å). At our standard level (PMP2/6-31G**/6-31G*+ZPC), the transition state is 56.5 kJ/mol above the reactants SC_2H_4 plus $SC_2H_4^+$ (and 180.7 kJ/mol above the dimer **h**). If single-point calculations are made at the PMP4/6-31G* level, the relative energy with respect to monomers decreases to 51.7 kJ/mol.

A search was made at the MCSCF level for the transition

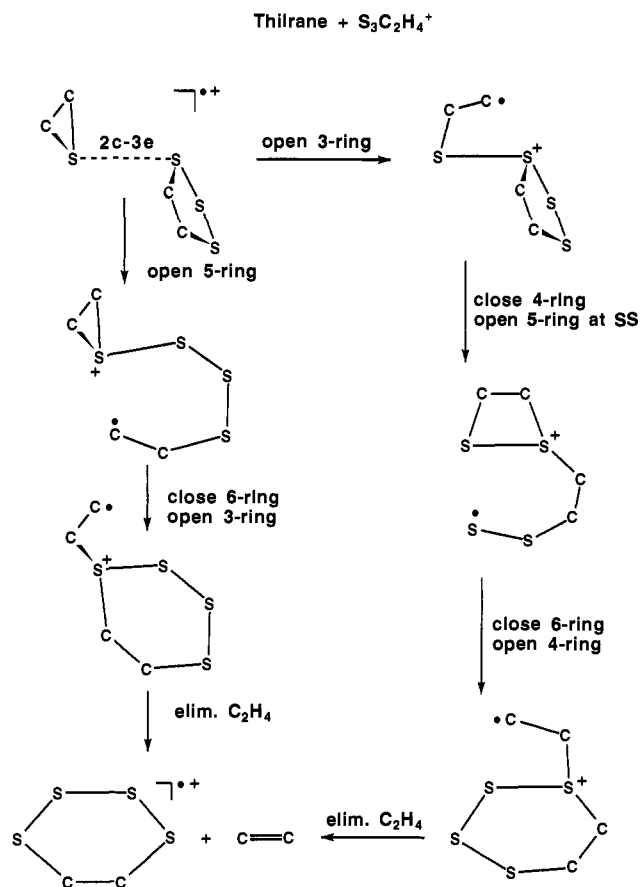
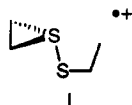


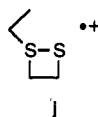
Figure 8. Reaction scheme showing two possible routes from the five-membered ring to the six-membered ring.

state, including the three orbitals and three electrons in a 3×3 complete active space. Unfortunately, the transition state could not be located at the MCSCF level. However, a single-point calculation at the CAS(3x3)/6-31G* level using the UHF/6-31G* geometry confirms the orbital picture presented above. CAS(3x3)/6-31G* calculations were also carried out at UHF/6-31G* geometries on the reactants SC_2H_4 plus $SC_2H_4^+$. Two alternative active spaces for the reactants, consisting of the bonding and antibonding S-C orbitals, are consistent with the CAS(3x3) used for the transition state. The first alternative consisted of CAS(2x2) for SC_2H_4 and ROHF for $SC_2H_4^+$ while the second alternative consisted of RHF for SC_2H_4 and CAS(3x3) for $SC_2H_4^+$. The first alternative was used since the total energy was 12.1 kJ/mol lower. At the CAS(3x3)/6-31G**/6-31G*+ZPC level, the transition state was 58.2 kJ/mol higher than monomers, which is almost unchanged from the PMP2 and PMP4 values. The wave function has large contributions from other configurations with the SCF configuration contributing 78%.

In ionized thirane, the barrier for S-C bond breaking must be at least as large as the endothermicity of the reaction $c-SC_2H_4^+ \rightarrow SCH_2CH_2^+$ which is 216.1 kJ/mol at our standard level (Figure 5). In comparison, the endothermicity of S-C bond breaking in the dimer is only 82.2 kJ/mol, because the bond order of the S-S bond increases as the S-C bond breaks. The experimental data presented above indicate that the dimer has a barrier to further reaction which is lower than dissociation back into monomers SC_2H_4 plus $SC_2H_4^+$. While the calculated barrier for S-C bonding breaking is currently higher than monomers, we believe that with further refinement (i.e. optimization at the MCSCF level) the barrier height will decrease. At present, the reverse activation barrier from the ring-opened form (**i**) to the dimer (**h**) is 98.5 kJ/mol.



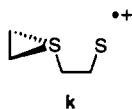
The first intermediate (i) has a normal S-S bond length (2.075 Å)²⁰ and nearly all of the spin density is on the terminal methylene. The second transition state occurs with the attack of the radical center on the second sulfur. One S-C bond is formed (2.345 Å in TSi/j) in the transition state while another S-C bond is broken (Figure 3, 2.242 Å).



The transition state TSi/j is 58.2 kJ/mol above i and 16.2 kJ/mol above reactant monomers. When the transition state and reactant monomers were reoptimized at the UMP2/6-31G* level and single-point calculations made at the PMP4/6-31G* level (with zero-point correction at the UHF/6-31G* level), the transition state was found to be 11.2 kJ/mol higher than reactant monomers. Transition state TSj/g was also found to have a spin-squared value higher than the expected value for a doublet ($\langle S^2 \rangle = 1.00$ (calc), 0.75 (expected), which may indicate that more refined methods may reduce the barrier height.

The product of the S-C bond forming/breaking reaction is a four-membered $S_2C_2H_4^+$ ring with an exocyclic CH_2CH_2 group. The geometry of the four-membered ring is very similar to the $S_2C_2H_4^+$ ion (g) proposed as the m/z 92 peak observed in the mass spectrometer. The majority of spin density resides on the terminal methylene group. The last step in the reaction mechanism is the simple cleavage of the exocyclic CH_2CH_2 group forming g plus ethylene (TSj/g). The C=C distance in the transition state TSj/g (1.373 Å) already shows considerable double-bond formation while the breaking S-C bond has increased to 2.552 Å. All other geometric parameters show very little change.

Another intermediate structure k, similar to i but with a terminal sulfur rather than a terminal carbon, was also found to be stable. The C_1 -symmetry structure is 108.0 kJ/mol more stable than reactants and only 16.2 kJ/mol less stable than the dimer h. However, it is difficult to envision a reaction pathway to k from the dimer h that does not have a high activation barrier. One possible route could be through intermediate i. The reaction would then not continue through TSi/j where the S-C bond of the three-membered ring opens as the four-membered ring is formed, but rather through a transition state where the S-S bond opens, since the only continuation from this intermediate that leads to observed products seems to be through intermediate j, no further calculations on the transition states were made.

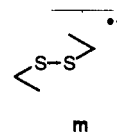


A third product structure l for m/z 92 was computationally found to be intermediate in energy between f and g. No intuitively obvious reaction pathway leading to this product could be envisioned, hence a detailed computational examination of the potential surface around this ion was not carried out.

A double ring-opened form of the thiirane dimer was calculated in C_i symmetry (m) and found to be 96.7 kJ/mol higher than reactant monomers (1 imaginary frequency). The very large

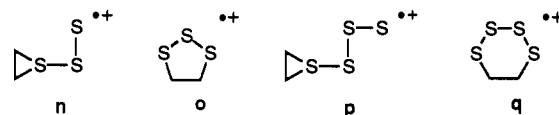


endothermicity indicates that this pathway would not be active in the mass spectrometer.



A summary of the potential energy surface calculated at the PMP2/6-31G*//6-31G*+ZPC is presented in Figure 4. All intermediates are lower in energy than the reactant monomers. The two transition states which are less stable than reactant monomers (TSh/i and TSi/j) both have a large degree of spin contamination and may benefit relative to monomers from more refined theoretical treatments. The alternative pathway to f plus ethylene is endothermic by 34.1 kJ/mol and cannot explain the experimental observations. Any activation barrier to formation of f (plus ethylene) in excess of the endothermicity would make the pathway even less likely.

Calculations have also been carried out for $S_3C_2H_4^+$ and $S_4C_2H_4^+$. The mechanism presented here would suggest that the sulfur atoms would be incorporated into a cyclic system. On the other hand, the mechanism presented by Baykut et al.⁷ would suggest that the sulfur atoms are added exocyclically.



At our standard level, the $C_2H_4SSS^+$ structure (n) is predicted to have a gauche orientation of the SSS linkage (C_1 symmetry) with respect to the three-membered ring, but a C_s structure is only 0.3 kJ/mol higher in energy. The five-membered ring (o) is predicted to have C_2 symmetry and was found to be 96.8 kJ/mol lower in energy than the C_1 structure (n).

Calculations for $S_4C_2H_4^+$ present a similar picture. A C_1 structure of $C_2H_4SSSS^+$ (p) was calculated to be 29.4 kJ/mol lower than a C_s structure. At the UHF/6-31G* level the six-membered ring (q) was found to be 18.3 kJ/mol less stable than the C_1 structure (p). However, inclusion of electron correlation favors the six-membered ring, and at our standard level the C_2 cyclic form (q) is 45.7 kJ/mol more stable than the C_1 structure (p) of $C_2H_4SSSS^+$. At the UHF/6-31G* level, one imaginary frequency was calculated for the C_2 structure, which indicates that a distortion to lower symmetry is favorable. Since the relative energy ordering of p and q changes upon inclusion of electron correlation, and given the fact that the six-membered ring is already more stable than $C_2H_4SSSS^+$, the lower-energy cyclic structure was not located.

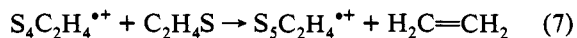
Since the five- and six-membered rings are lower in energy than the structures with exocyclic sulfurs, we suggest that ring expansion takes place. Figures 7 and 8 show two possible mechanisms leading to the rings o and q. The first mechanism is essentially a straight analogy of the proposed mechanism of the formation of m/z 92. The second mechanism involves more steps but allows for the initial opening of the more strained ring in the system.

Conclusion

The reaction surface involving m/z 60, 120, 92, 124, and 156 was reinvestigated with emphasis on finding exothermic reaction pathways leading to m/z 92, 124, and 156. Though structure g

(the four-membered ring at m/z 92) had previously been proposed as a reasonable species it was discarded without the aid of theoretical calculations in favor of **f**. As stated, we were led to question the participation of **f** in the ethylene extrusion reaction in light of our experimental high-pressure mass spectra. Our calculated potential energy surface shown in Figure 4 demonstrates that **g** plus ethylene is 43.0 kJ/mol more exothermic than reactants and 77.1 kJ/mol more stable than **f** plus ethylene. Shown in Figure 4 are three stable intermediate structures **h**, **i**, and **j** and three transition states TSh/**i**, TSi/**j**, and TSj/**g** on the reaction path to **g** (m/z 92) and ethylene. The first transition state is 56.5 kJ/mol more endothermic than reactants and thus would seem to vitiate the reaction mechanism. However, the transition state showed substantial spin contamination and its stability may be underestimated. It is worth noting that all the intermediate structures as well as the final products on the potential energy surface are exothermic with respect to reactant monomers. Under our experimental conditions the nascent association product **h** contains enough internal energy to proceed along the reaction path to products **g** and ethylene. As the temperature is lowered and the pressure increased (conditions which favor energy removal and association reactions), **h** is stabilized and the m/z 120 intensity increases.

The mass spectra reported here and those from the earlier ICR work show sequential reactions of m/z 92 with thirane followed by elimination of ethylene yielding m/z 124 and 156 (reaction 3 and reaction 4) but no m/z 188. m/z 124 and 156 have previously been assigned as **n** and **p**. We suggest that m/z 124 and 156 may actually be **o** and **q**, the ring expanded species. Since our conditions (higher pressure and a wider temperature range) should greatly promote ion-molecule reactions relative to typical ICR conditions, we postulate that further expansion of the ring in **q** to a seven-membered ring is unfavorable and hence our proposed reaction sequence for ring expansion ends at reaction 4 and reaction 7 does not take place.



Acknowledgment. We thank Dr. Tom Webb for carefully reading and reviewing this manuscript and Mary James for rechecking the mass spectra. A.J.I. also thanks the donors of the Petroleum Research Fund, administered by the American Chemical Society, and the Auburn University Chemistry Department for financial support. We also thank the Alabama Supercomputer Network and the NSF supported Pittsburgh Supercomputer Center for a generous allocation of computer time.